Multiband Metamaterial Absorber with a Negative Permeability

Khedidja BOURAS[1], Abdelhadi LABIAD[1], Mouloud BOUZOUAD[1]

[1]Telecommunication Signals and Systems Laboratory University of Laghouat, BP 37G, Road of Ghardaïa, 03000 Laghouat, Algeria

E-mail: kh.bouras@lagh-univ.dz

Abstract **-** In this work, a multiband frequency metamaterial absorber is designed. The structure is made of a several of frequency selective metasurfaces, each one consists of a periodic arrangement identical unit cells. These layers have two different behaviors that depends on an external control system (ON/OFF) state, this latter represented by a switches integrated in each unit cell, where the open switch state (OFF) for the disconnected cross type metamaterial that behaves as an absorbent medium, and an closed switch state (ON) for the connected cross type metamateral that behaves as a conducting medium, based on these agile layers we can control the frequency band of the absorber structure.

Keywords **-** Metamaterials; Multiband of absorption; Stealth; Multi layer, Agile Metamaterial Cell.

I. Introduction

In recent years, metamaterial absorber has attracted the attention of many researchers in many areas of applications, including renewable energy [1], sensor [2, 3], stealth technology [4-7], reduction of radar cross section [8, 9].

In this work, we use a cross type metamaterial unit cell controllable through the switch installed at the end of the cross branches as depicted in Fig. 1[10]

According to the switches stats (ON/OFF) the unit cell have two behaviors as shown in Fig 2. If the switches are open (OFF-stat) each cross is disconnected with his four neighbors (disconnected cross type metamaterial) and the metamaterial behaves as a resonance absorber medium. Otherwise, the switches are closed (ON-stat) and each cross is connected to four neighbors (connected cross type metamaterial) and the metamaterial behaves as conducting medium. The addition of a ground plane in the first substrate will improve the absorption of the cell and the characteristic impedance increasing, by stacking the layers one above each other every time the absorption value enhanced and the characteristic impedance, by stacking the layers one above each other, in every time the absorption value enhanced and the characteristic impedance decreasing. In the first time we set just the first layer in the connected type, and we keep the rest of the disconnected type without changing the state of the bottom ground plan, in the second time we set the two first layers in the connected type, and we keep the rest of the disconnected type until we arrive to the sixth layer, and so we have got six cases in each case we have a different frequency absorption band.

II. Cross Type Metamaterial Absorber Structure

The proposed metamaterial unit cell is designed to operate at 40 GHz. This latter is a metal cross connected or disconnected deposited at the top of a dielectric substrate type (FR4 epoxy) with a permittivity constant $\varepsilon_r = 4.4$. The dimensioning of the unit cell is dictated by the homogenization hypotheses that there dimensions must be much smaller than the working wavelength for the homogenization conditions to be verified. The geometry and dimensions of the unit cell structure are shown in Fig. 1.

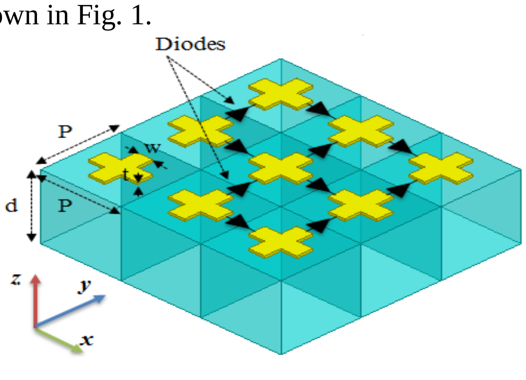

Fig. 1. Metamaterial structure geometry of one metamaterial layer (P = 2, d = 2.4, w = 0.7, t = 0.035, g = 0.5 (all dimensions in mm).

To extract the effective parameters unit cell from the S parameters, when the Master and slave walls are applied along the X and Y axes using HFSS software, while the incident wave is oriented along the Z axis. Figure 2-(a) shows negative permeability of -6.5 at 36.85 GHz.The negative value of the real part starts at the frequency of 36.1GHz , where also appears the plasma frequency of the permittivity real part shows in figure 2-(b), while the magnetic loss at its highest value, which reaches to 11 then decreases until it close to zero. The effective refractive index real part is negative and begins closing to zero from 38 GHz, whereas its imaginary part is positive which varies between 2 and 6 as the figure 2-(c) shows.

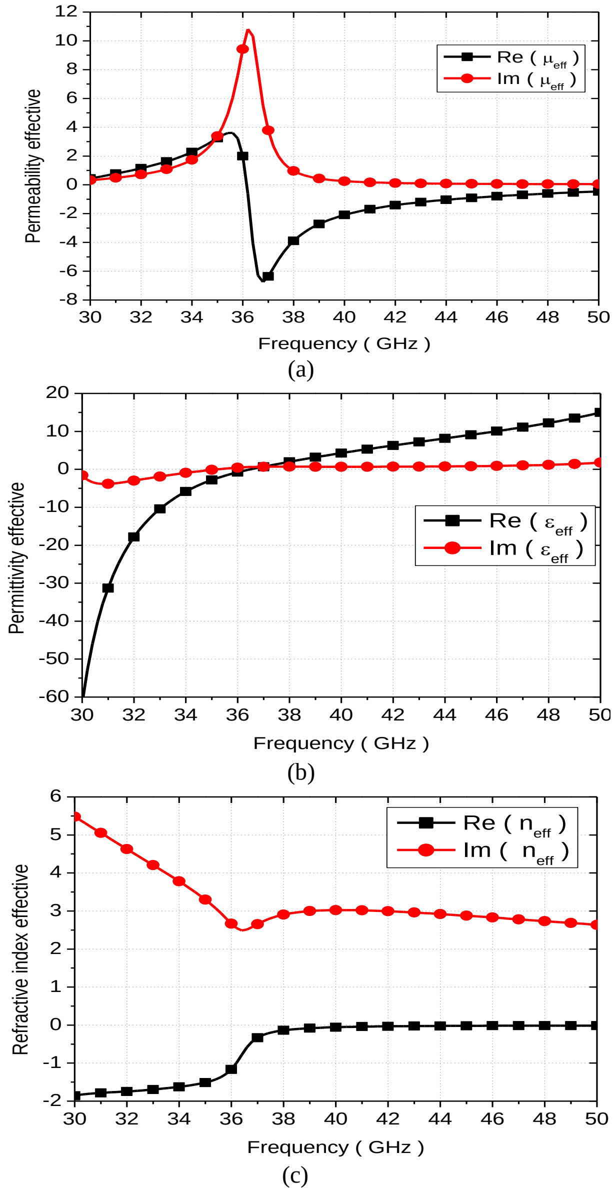

Fig. 2. Metamaterial unit cell disconnected type effective constitutive parameters : (a) effective permeability, (b) effective permittivity, and (c) effective refractive index

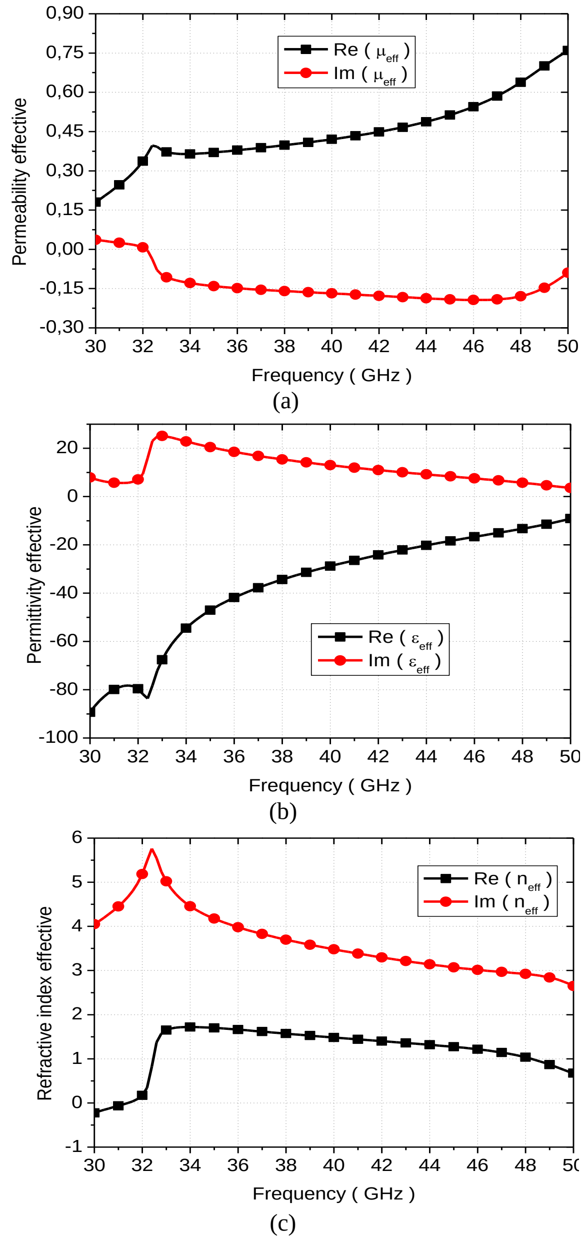

Fig. 3. Metamaterial unit cell connected type effective constitutive parameters : (a) effective permeability, (b) effective permittivity, and (c) effective refractive index

According the effective constitutive parameters represented in Fig. **3**, the connected unit cell type exhibit a negative permittivity and a near to zero refractive index, for that this type can behave as a conducting medium

III. MULTIBAND METAMATERIAL ABSORBER DESIGN

The absorber structure is obtained by stacking several metasurfaces layers and adding a ground plan in the bottom of a structure to prevent the passage of the incident waves. The connected cross type metamaterial behaving as conducting medium can play the role of a controllable ground plane. Finally, we can see the absorber structure as an arbitrary stacking of several connected or disconnected metamaterial layers where the bottom one is obligatory a connected type metamaterial as shown in Fig. 3.

Once incident electromagnetic waves arrive at the air-absorber interface, there will be a concentration of energy between two metamaterial layers and the waves are trapped inside the metamaterial layers and remain resonating until disappearing in the form of heat.

In order to achieve a perfect absorption, the transmission and the reflection energies should be close to zero as the equation (3) shows, where $A(\omega)$ the absorption energy is, $R(\omega) = |S_{11}|^2$ is the reflection energy, and $T(\omega) = |S_{21}|^2$ is the transmission energy.

$$R = \frac{Z_c - Z_0}{Z_c + Z_0} \quad (1)$$

$$Z_c = Z_0\sqrt{\frac{(1+S_{11})^2}{(1-S_{11})^2}} \quad (2)$$

$$A(\omega) = 1 - R(\omega) - T(\omega) \quad (3)$$

The presence of the ground plan at the bottom of the absorber ensure transmission coefficient close to zero. According to equations (1) and (2) which show the relationship between the coefficient of reflection and the characteristic impedance of the material, it is necessary to look for metamaterial impedance close to that of the free space $Z_0 = 120\pi \approx 377\,\Omega$, to minimize the reflection energy.

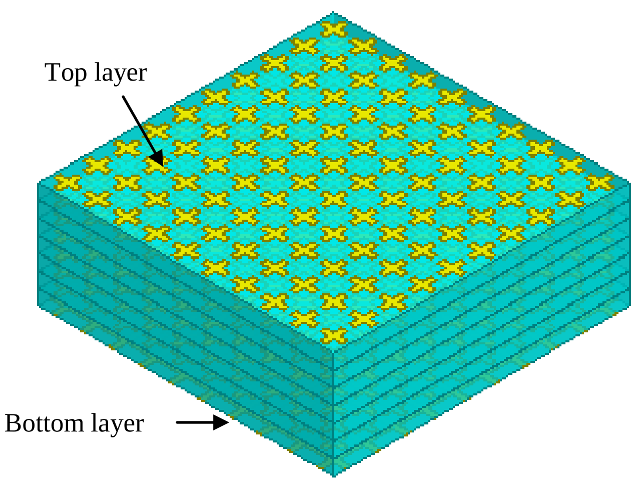

Fig. 4. Multilayer absorber (seven stacked of metamaterial unit cells)

In order to increase the absorption value and bandwidth of the structure, several identical unit cells are stacked until the characteristic impedance reaches the free space value.

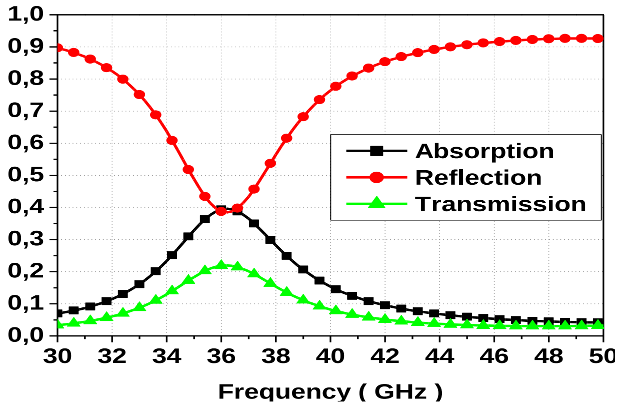

Fig. 5. Absorption, reflection, and transmission parameters of unit cell

Fig. *5* shows that the absorption of the incident waves in one metamaterial layer is very low, of the order of 40%. From Fig. 6, it appears that the metamaterial characteristic impedance is very great compared to that of the free space which leads to a great reflectivity at the interface. From Fig. 7 it appear clearly that the metamaterial impedance characteristic goes close to the free space impedance (Z_0) when the number of layers forming the absorber increases. Not that with seven layers of metamterial the absorber characteristic impedance reaches the value of 422 Ω. Fortunately this increase of the layers number leads also to an increase in the absorption frequency bandwidth according to Dallanbach layer approach [11] Fig. 8.

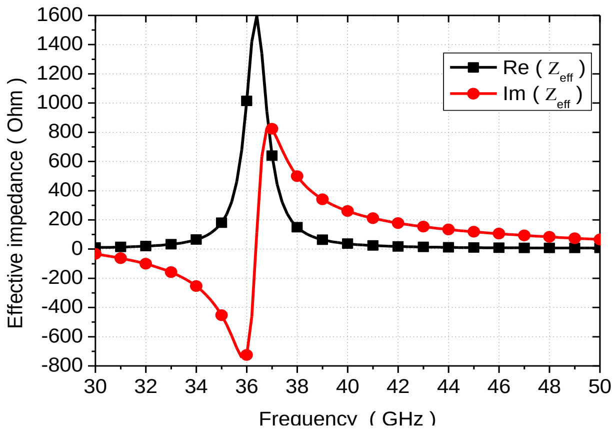

Fig. 6. The characteristic impedance of one unit cell

The absorber structure that allows reaching characteristic impedance close to that of the free space is obtained by stacking seven layers of metamaterial where the bottom one is made of connected cross type and the seven others are made of disconnected cross type. As shown in Fig. **4**, this structure presents four absorption bands: B1 = [32.06 - 33.05], B2 = [34.82 - 36.2], B3 = [37.5 - 39.3], and B4 = [39.92 - 44.74]. The absorption ratio of the metamaterial multiband absorber increases with the frequency. It starts from 84.75% at 32.6 GHz (frequency band B1) and reaches value of 97.58 % at 43 GHz (B4). For the bands B2 and B3 the absorption is 90.52% and 93.41% at respectively 35.4 GHz and 38.4 GHz.

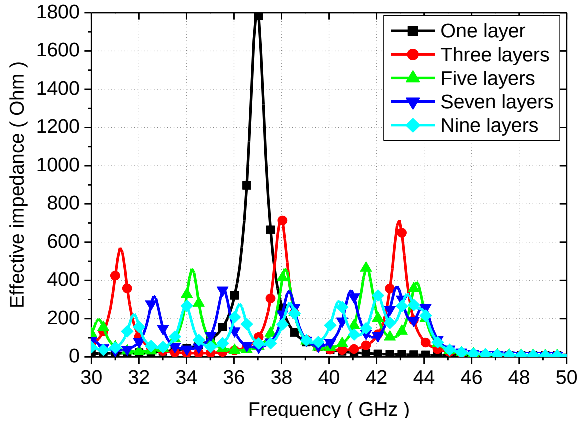

Fig. 7. The characteristic impedance of metamaterial structure from one cell until seven unit cross.

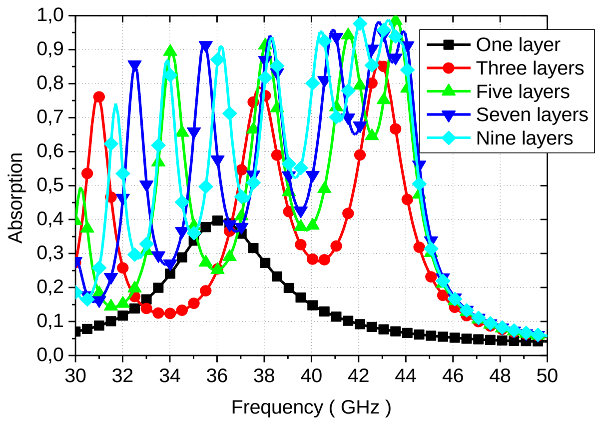

Fig. 8. Absorption of the multilayer metamaterial absorber

IV. POLARIZATION AND INCIDENCE WAVES

In order to obtain the angle variation phi, the antennas are turned around the z-axis. Due to symmetry in XY plan, to obtain the theta angle of the incident wave, the antennas can be turned around the y-axis, for example, as shown in **Fig. 9**. The behavior of structure doesn't change with phi due to geometric symmetry of the structure in XY plan. The absorber absorption changes with theta.

The absorption is maximal for $\theta = 0^0$, where the propagation direction is normal to the metamaterial motif (the cross), and null for $\theta = 90^0$, where the direction of propagation of incident wave is parallel to the metamaterial motif. In the layer case the incident waves don't see the conducting crosses and face only the absorber medium. The operating frequencies are slightly the same and don't change with the polarization angle of the incident wave.

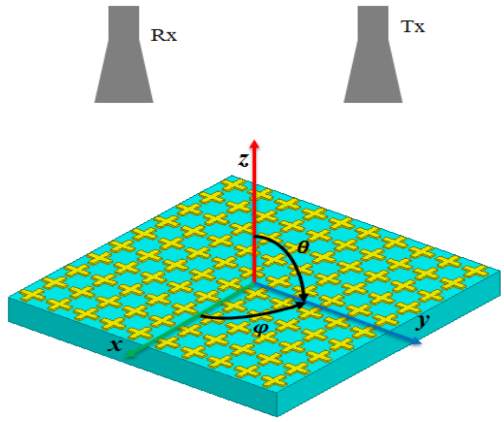

Fig. 9. Axes and angles representation of variation for incidence waves

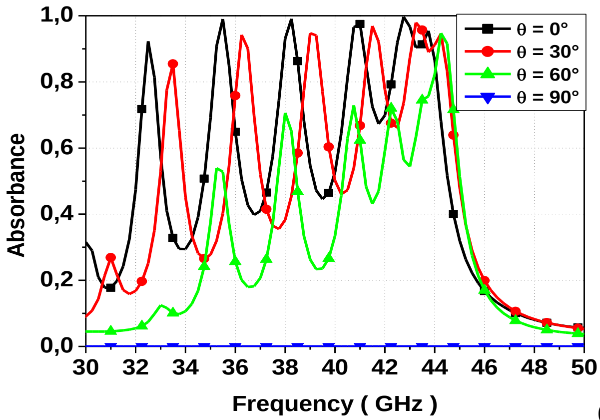

(a)

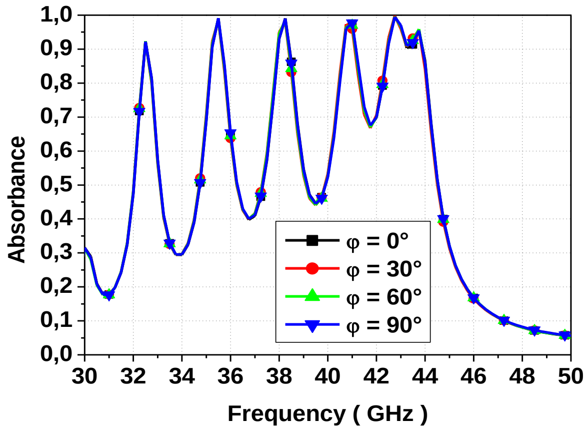

(b)

Fig. 10. Absorption variation with the incident wave polarization: (a) Phi =0 and different values of theta, (b) Theta = 0 and different values of phi.

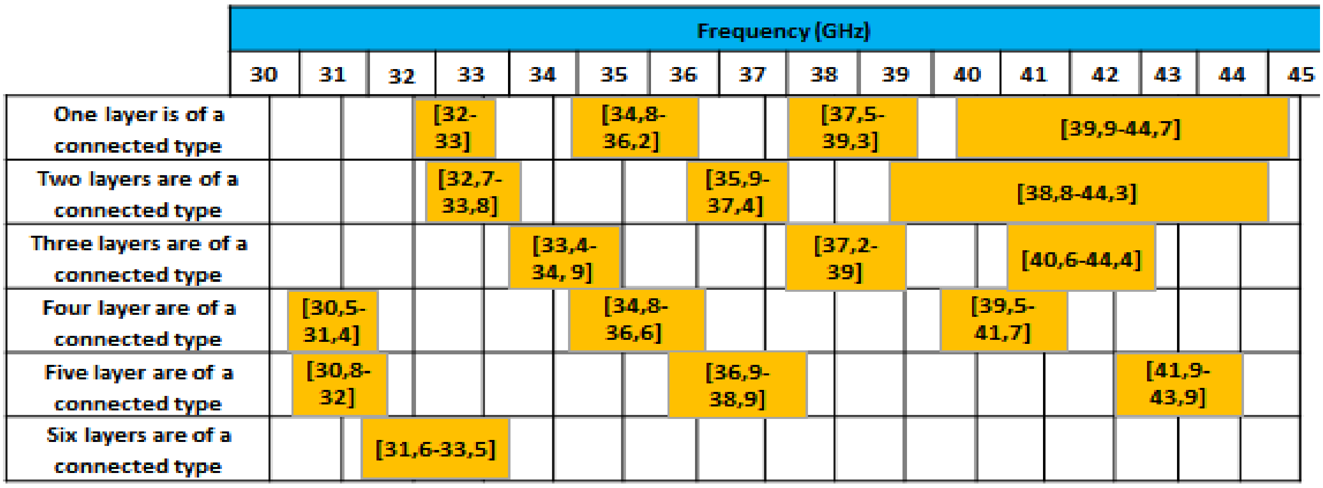

Fig. 11. Presentation of bandwidth of absorption in each case.

V. ABSORPTION FREQUENCY BAND CONTROL

The absorption frequency band control is obtained by controlling the behavior (connected/disconnected cross type metamateial) of each of the seven layers constituting the absorber. We have six different configurations.

In each one the N^th first layers are based on the connected cross type metamaterials and the remaining ones based on the disconnected cross type metamaterials, where N varies from 1 to 6.

Fig. **11** summarizes the absorption frequency band of the multiband metamterial absorber.
The first frequency absorption band (B1) can be controlled by increasing the number of the connected type layers (n_c). Indeed, when n_c increases the band B1 shifts to high frequencies from 32.5 to 38GHz and his width increases from 1 GHz to 2 GHz. We not also that last absorption frequency band (B4) has large width greater than 4 GHz except for the case where $n_c = 5$. B1 appear cutoff frequency is constant and equal to 44.5 GHz while the lower cutoff frequency varies slightly from 39 to 42 GHz.

VI. CONCLUSION

We are interested by designing of unit cell controlled by an external switching system and which exhibits two different behaviors depending on the switches states (ON or OFF). If the switches are open (OFF) so the unit cell behaves like a absorbent material which is the disconnected cross type metamaterial and if the switches are close (ON) then the unit cell behaves like a conductor material which is the connected cross type metamaterial. The multiband frequency metamaterial absorber structure proposed composed of several layers of controllable metasurfaces. Absorber multilayer designs present wide bandwidths and an appropriate impedance matching with the free space. The width of the absorption bands depends on the number of the meta-material layers. The position of a certain absorption frequency bands can be controlled by the number of connected cross type layers from the bottom to the top layer without change the state of the ground plan. Using a structure of seven layers the first band B1 is shifted from 32.5 to 38GHz with increasing in the bandwidth frequency estimated by 1 GHz by controlling the number of connected cross layers type.

VII. REFERENCES

[1] P. Rufangura, C. Sabah “Perfect metamaterial absorber for applications in sustainable and high-efficiency solar cells”., *Journal of Nanophotonics*, April 2018.

[2] Y. Zhang, J. Zhao , J. Cao, and B. Mao “Microwave Metamaterial Absorber for Non-Destructive Sensing Applications of Grain” *Sensors* Published: 12 June 2018.

[3] M. Karaaslan, E. Unal, O. Akgol, C. sabah, “Microwave metamaterial absorber for sensing applications”, *Opto-Electronics Review* 25(4), November 2017.

[4] K. Iwaszczuk, A. Strikwerda, K. Fan, X. Zhang, R. Averitt, and P. Jepsen, "Flexible metamaterial absorbers for stealth applications at terahertz frequencies"., *Optics Express* Vol. 20, Issue 1, pp. 635-643. 2012.

[5] J. Kim, K. Han and Jae W. Hahn, "Selective dual-band metamaterial perfect absorber for infrared stealth technology,"*scientific reports* Article number: 6740 2017.

[6] Y. Shen, J. Zhang, Y. Pang, J. Wang, H. Ma, and S. Qu, "Transparent broadband metamaterial absorber enhanced by water-substrate incorporation," *optics express* Vol. 26, Issue 12, pp. 15665-15674. 2018.

[7] K. Iwaszczuk, K. Fan, A. C. Strikwerda, X. Zhang, Averitt, D. Richard Jepsen, Peter Uhd, "Stealth metamaterial objects characterized in the far field by Radar Cross Section Measurements" *International Workshop on Optical Terahertz Science and Technology*, 2011.

[8] Li, S. J. et al. "Ultra-broadband Reflective Metamaterial with RCS Reduction based on Polarization Convertor, Information Entropy Theory and Genetic Optimization Algorithm.", *Scientific reports*. 6, 37409, 2016.

[9] J. Chen, Q. Cheng , J. Zhao, D. Sha Dong, and T. J. Cui "Reduction of Radar Cross Section Based on a Metasurface"., *Progress In Electromagnetics Research*, Vol. 146, 71–76, 2014.

[10] C. Saleh, M. bouzouad, "Metamaterial patch antenna radiation pattern agility'., Applied *Physics* A 115(2), October 2013.

[11] Jens Reinert Jannis Psilopoulos Jens Grubert Arne F. Jacob "On the potential of graded-chiral Dallenbach absorbers", *Microwave and optical technology letters* 16 July 2001